

# Anisotropy of photocurrent for two-photon absorption photodetector made of hemispherical silicon with $(\bar{1}10)$ plane

B. Shi · X. Liu · Z. Chen · G. Jia · K. Cao · Y. Zhang ·  
S. Wang · C. Ren · J. Zhao

Received: 12 June 2008 / Revised version: 23 September 2008 / Published online: 30 October 2008  
© Springer-Verlag 2008

**Abstract** We fabricated a hemispherical nearly-intrinsic Si-based photodetector with  $(\bar{1}10)$  plane. The photocurrent generated from the detector under a continuous wave laser at the wavelength of 1.3  $\mu\text{m}$  was observed. The photocurrent shows a quadratic dependence on the incident optical power. The dependence of the photocurrent on the azimuth of the incident optical field is consistent with the anisotropy of the two-photon absorption in Si crystals. The ratio of the two nonzero independent components of the third-order susceptibility of silicon is obtained to be 0.42 from the observed result of the anisotropy of the photocurrent.

**PACS** 42.65.-k · 78.40.Fy · 42.25.-p

## 1 Introduction

Silicon photonics has attracted much attention recently because of its potential applications in the near- and mid-infrared regions. Silicon exhibits a significant nonlinearity in the devices of p–n diode, waveguide, photodiode, avalanche diode, and luminescent diode for autocorrelation measurements [1, 2]. Two-photon absorption (TPA) in semiconductors is an attractive alternative to second-harmonic

generation (SHG) for autocorrelation [3–5] because of potential lower cost (compared to the use of photomultiplier (PM) tube), increased sensitivity, and ease of use resulting from having a wide wavelength range of operation without needing the adjustment of crystal tilt angle for phase matching of a nonlinear crystal for SHG. It is obviously significant to fabricate TPA photodetectors with high sensitivity used in the measurements of optical autocorrelation.

Silicon is a kind of centrosymmetric crystals; it does not have any second-order nonlinear optical effects in its bulk at dipole approximation. The third-order nonlinear response is generally anisotropic, unlike the isotropic nature of the linear optical effects. The anisotropy of third-order susceptibility  $\chi^{(3)}$  of silicon is typically studied through third-harmonic generation and four-wave mixing. J. Zhang et al. [6] has recently reported the result of the anisotropy of  $\chi^{(3)}$  employing the method of z-scan. We have observed the anisotropy of  $\chi^{(3)}$  of silicon crystals from the viewpoint of the anisotropy of photocurrent generated from a silicon hemispherical photodetector. By choosing specific crystal orientations and wave-vector propagation directions, different third-order tensor susceptibility elements can be determined [7]. We have studied the anisotropy of  $\chi^{(3)}$  based on the  $(\bar{1}10)$  surface of silicon.

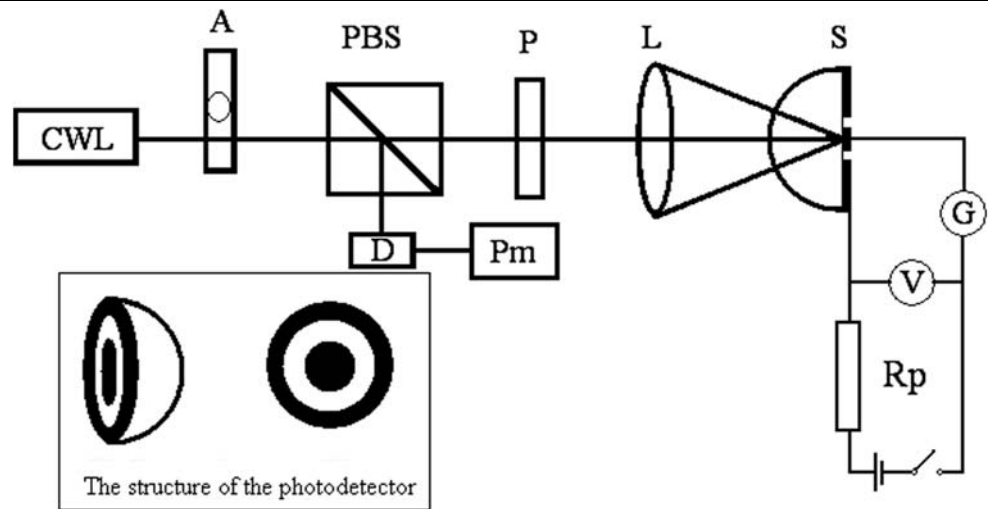
In this letter, we present the hemispherical nearly-intrinsic Si-based photodetector with  $(\bar{1}10)$  plane operating at 1.3  $\mu\text{m}$  wavelength from a continuous wave laser. First, we measured the quadratic dependence of the photocurrent on the incident optical power and its nonlinear dependence on the bias voltage. Next, we measured the anisotropy of the photocurrent versus the azimuth of the incident optical field and deduced the anisotropy of the third-order susceptibility of silicon.

B. Shi · Z. Chen · G. Jia (✉) · K. Cao · Y. Zhang · S. Wang ·  
C. Ren · J. Zhao  
State Key Laboratory on Integrated Optoelectronics, College  
of Electronic Science and Engineering, Jilin University,  
2699 Qianjin Street, Changchun 130012, China  
e-mail: [jiagang@jlu.edu.cn](mailto:jiagang@jlu.edu.cn)  
Fax: +86-431-85168270

X. Liu  
College of Communication Engineering, Jilin University,  
5372 Nanhu Road, Changchun 130012, China

**Fig. 1** A schematic diagram of the experimental system.

CWL: 1.3  $\mu\text{m}$  continuous wave laser; A: optical attenuator; PBS: polarized beam splitter; P: half-wave plate for 1.3  $\mu\text{m}$ ; L: objective lens; S: nearly-intrinsic Si hemispherical photodetector; G: galvanometer; V: voltage meter;  $R_p$ : protective resistance; D: Ge detector; Pm: optical power meter. The inset shows the structure of the photodetector, and the shadows represent the electrodes



## 2 Experimental setup

As shown in the inset of Fig. 1, the detector was made of nearly-intrinsic silicon crystal with resistivity of  $6000 \Omega \cdot \text{cm}$  and made into a hemisphere with a radius of 3 mm. The Si hemisphere was used as both a detector and a solid immersion lens (SIL) in the experiments. The bottom of the detector is  $(\bar{1}10)$  plane, on which aluminum electrodes were evaporated. The electrodes consisted of concentric circular and annular metal contacts with a spacing of 0.15 mm and a radius of 0.5 mm for the central electrode. The contacts between the aluminum and the silicon hemisphere are considered to be ohmic contacts. Because TPA would substantially occur in the vicinity of the focused spot (the center of the hemisphere), the concentric electrodes could collect the photo-excited carriers efficiently.

Figure 1 schematically shows the experimental system. The light source was a continuous wave (cw) solid laser with a wavelength of 1.3  $\mu\text{m}$ . The optical attenuator controlled the optical power. The polarized beam splitter divided the incident beam into two beams, one beam was coupled into the Ge detector for monitoring optical power by the optical power meter, the other beam passed through the half-wave plate and the objective lens, and focused at the center of the hemisphere. The polarization of light was altered by the rotation of the half-wave plate about its surface normal. The work distance of the  $12\times$  objective lens is about 6 mm and NA is 0.3 in the free space.

## 3 Experimental results and analyses

A measurement of the photocurrent dependent on the incident optical power was carried out initially. The Si hemisphere was biased at 1 V. The measured photocurrent shows a quadratic dependence on the incident power, as shown in

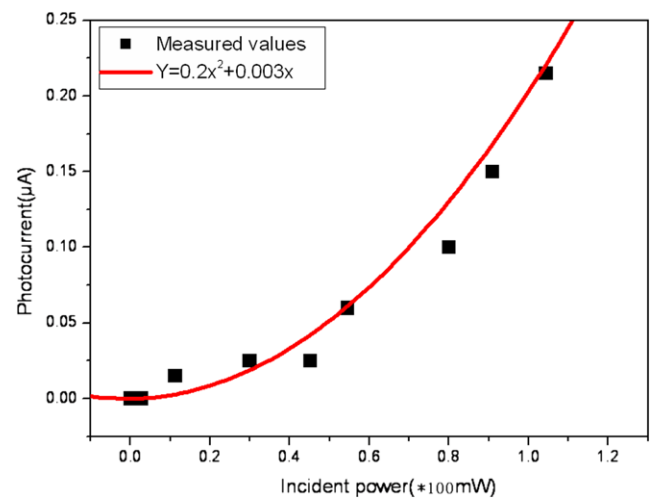


**Fig. 2** Photocurrent versus incident power. Bias voltage at 1 V for the detector

Fig. 2, which indicates the nonlinear absorption in the Si hemisphere. Although the labeled power of the cw laser was 200 mW, the factual incident power on the detector in the experiments was measured to be about 100 mW. Here, we simply define the responsivity of the detector as the ratio of the photocurrent to the incident optical power, and it is different at different power since the photocurrent is quadratically dependent on the incident power. We chose the maximal optical power as 100 mW, and computed the responsivity of the detector at the given power to be about  $2 \mu\text{A}/\text{W}$  at 1 V bias, which was comparable to the powers of the TPA devices responding to laser pulses [8].

The responsivity of the hemispherical photodetector responding to laser pulses will be higher than that responding to cw lasers. The higher responsivity is attributed to the role of hemispherical SIL [9].

The dependence of the photocurrent on the bias voltage was also measured under a fixed optical power of about

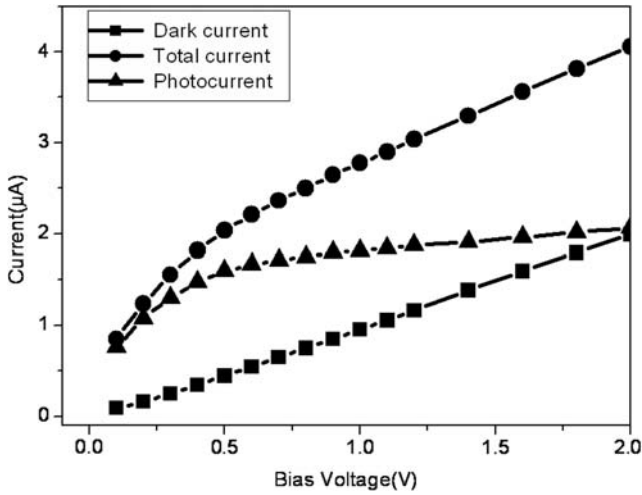


**Fig. 3** Photocurrent against bias voltage. The *squares* stand for the dark current; the *filled circles* for the total current; and the *triangles* for the photocurrent. The incident optical power on the detector was about 100 mW

100 mW. The result is shown in Fig. 3. The quite slow increase of the photocurrent after 1 V bias indicates the near saturation of the photocurrent with increasing bias. This behavior of the photocurrent is in agreement with the characteristic of TPA which is typically saturated with the increasing bias [8]. In TPA theory, the density of photo-generated carriers is determined by the fixed incident optical intensity, and the mobility of photo-generated carriers is constant under weaker biased electric fields, but the mobility will decrease under stronger fields and the photocurrent is nearly saturated.

Figure 4 shows dependence of the photocurrent on the azimuth, the solid line is the fit to the data, the fitted result is

$$i = 1.53 \times 10^{-6} \times \left( 1 + 2 * (-0.25) \left( \frac{3}{32} \cos(4(\alpha - 55)) + \frac{1}{8} \cos(2(\alpha - 55)) - \frac{7}{32} \right) \right), \tag{1}$$

where  $\alpha$  is the angle of the polarization of the optical electric-field with respect to the [111] orientation. Equation (1) reflects the anisotropy of TPA in the detector. The analysis is given below.

When an intense light beam traverses semiconductor, TPA can become the dominant loss mechanism if the light is sufficiently intense and  $\hbar\omega < E_g < 2\hbar\omega$ , where  $E_g$  is the energy gap and  $\hbar\omega$  is the incident photon energy. As the light was propagating along the  $z$ -axis direction, a spatial and temporal integration intensity  $I(z, t)$  would decrease because of linear loss single-photon absorption (SPA) and TPA:

$$\frac{dI(z, t)}{dz} = -\alpha I(z, t) - \beta I^2(z, t), \tag{2}$$

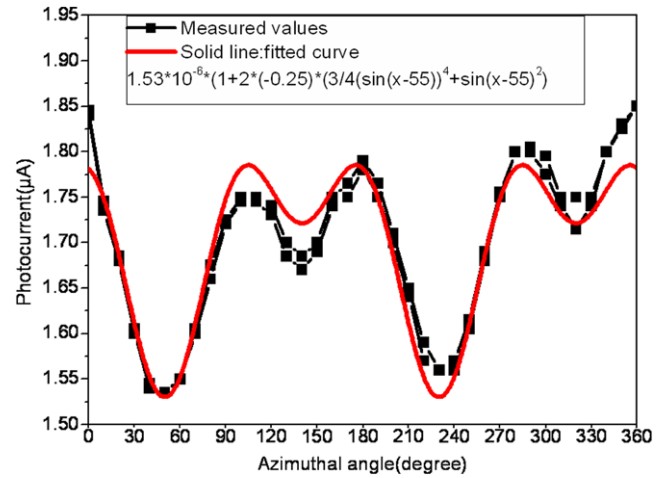


**Fig. 4** Photocurrent versus azimuth of optical field. The detector was biased at 1 V and under optical excitation of about 100 mW. The increment of the half-wave plate angle is  $5^\circ$

where  $\alpha$  is the linear loss SPA coefficient and  $\beta$  is the TPA coefficient.

For the wavelength of 1.3  $\mu\text{m}$ , the linear loss SPA in silicon is approximately negligible because single photon energy is not sufficient enough to excite any interband transitions in nearly-intrinsic Si crystal. So the nonlinear absorption TPA is dominant in the silicon hemisphere at the wavelength of 1.3  $\mu\text{m}$ .

The TPA induced photocurrent may be described by [8]

$$J_{\text{TPA}} = \frac{N_p e}{2} \eta, \tag{3}$$

where  $N_p$  is the number of photons absorbed per second and  $e$  is the electron charge. The conversion efficiency of the hemispherical detector, denoted by  $\eta$ , is defined by the ratio of the detected electrons to the half of the absorbed photons inside the hemisphere.

The TPA coefficient is related to the imaginary parts of effective third-order susceptibility  $\chi_{\text{eff}}^{(3)}$  described by [10]

$$\beta = \frac{3\omega}{2\epsilon_0 c^2 n_0^2} \text{Im} \chi_{\text{eff}}^{(3)}(\omega; -\omega, \omega, \omega), \tag{4}$$

where  $\epsilon_0$  is the dielectric permittivity in vacuum,  $n_0$  the polarization-independent refractive index of the medium, and  $c$  is the speed of light in vacuum.

As silicon crystals belong to the  $m\bar{3}m$  point-symmetry group, the third-order susceptibility  $\chi^{(3)}$  of this group has only two independent components, namely,  $\chi_{1111}^{(3)}$  and  $\chi_{1122}^{(3)}$  [7]. Note that this is true for both real and imaginary parts of  $\chi^{(3)}$ . When the incident light is propagating parallel to the  $[\bar{1}10]$  crystallographic axis, the optical electric-field will be parallel to the  $(\bar{1}10)$  plane and is given by  $\vec{E} = E_0(\cos\theta\hat{x} + \sin\theta\hat{y})$ , where  $\theta$  is the angle of the optical electric-field with respect to the [001] crystallographic axis,

$\hat{x}$  and  $\hat{y}$  denoting the unit directions of the [001] and [110] orientations, respectively. The form of the third-order susceptibility for the  $m\bar{3}m$  point-symmetry group is as the same as that of the  $\bar{4}3m$  point-symmetry group. Therefore, for this specific geometry, the effective third-order susceptibility is expressed as [11]

$$\chi_{\text{eff}}^{(3)}(\theta) = \chi_{1111}^{(3)} \left[ 1 + 2\sigma \left( \frac{3}{4} \sin^4 \theta - \sin^2 \theta \right) \right], \quad (5)$$

where  $\sigma$  is the coefficient of anisotropy defined by

$$\sigma = \frac{\chi_{1111} - 3\chi_{1122}}{\chi_{1111}}. \quad (6)$$

For a fixed incident optical intensity, the intensity of photocurrent is proportional to the coefficient of TPA. We can obtain accordingly

$$\begin{aligned} J_{\text{TPA}} &\propto \chi_{\text{eff}}^{(3)} \\ &= \chi_{1111}^{(3)} \left( 1 + 2\sigma \left( \frac{3}{32} \cos(4\theta) + \frac{1}{8} \cos(2\theta) - \frac{7}{32} \right) \right). \end{aligned} \quad (7)$$

Equation (1) is in good accord with the TPA theory expressed as (7). From (1), we can deduce the anisotropy of  $\chi^{(3)}$ . In our case,  $\sigma = (\chi_{1111} - 3\chi_{1122})/\chi_{1111} = -0.25$ , thus we can obtain  $\chi_{1122}^{(3)}/\chi_{1111}^{(3)} = 0.42$ . This value is very close to the result measured in [6] and [12]. In [6], the authors used the z-scan method to obtain the anisotropy  $\sigma$  by relatively complicated computations.

We also used a cw solid laser with a wavelength of 650 nm and a power of 4.5 mW to excite the hemispherical Si detector. Figure 5 shows the linear dependence of the photocurrent induced by single photon absorption on the incident optical power. We observed that the photocurrent induced by SPA was independent of the azimuth, as shown in the inset of Fig. 5. We consider that the two exceptional values of 3.05  $\mu\text{A}$  at 75° and 105° in the inset are due to measuring errors. This observed result confirms the TPA anisotropy in the hemispherical Si photodetector.

In our case, the anisotropy of the third-order susceptibility is obtained directly by the measured anisotropy of the photocurrent. If the bottom of the Si hemisphere is chosen as the (111) plane, and the wave-vector propagation direction is along the [111] orientation, the effective third-order susceptibility will be independent of the azimuth of the optical field. The experiment for this case is under investigation. Photodetectors with this specific geometry are more useful in practice because the photocurrent is independent of polarization. We are developing the photodetector products.

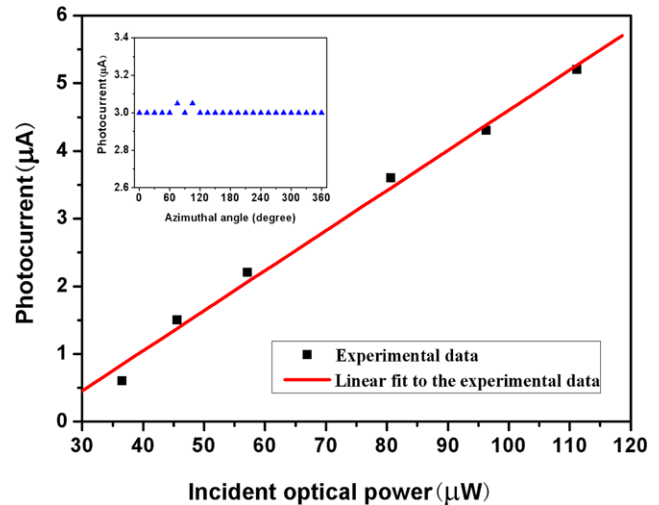


**Fig. 5** Photocurrent against incident optical power. The detector was biased at 5 V. The abscissa just indicates the power monitored by the optical power meter, not the actual power incident on the fabricated detector. The inset shows the independence of the photocurrent from the azimuth

## 4 Conclusions

We have presented the hemispherical nearly-intrinsic Si TPA photodetector with ( $\bar{1}10$ ) plane operating at wavelength of 1.3  $\mu\text{m}$  from a cw laser. The responsivity of the detector was about 2  $\mu\text{A}/\text{W}$  at 1 V bias. Compared to the waveguide photodetector, the hemispherical solid immersion lens improved the response sensitivity effectively. The dependence of the photocurrent on the azimuth of the optical electric field is consistent with the anisotropy of TPA in Si crystals. Furthermore, the ratio of the two nonzero independent components of the third-order susceptibility of silicon crystals  $\chi_{1122}^{(3)}/\chi_{1111}^{(3)}$  is about 0.42, deduced from the anisotropy of the photocurrent. The high sensitive hemispherical Si photodetector is easy to fabricate and is useful in autocorrelation for measuring ultrashort laser pulses with wavelengths in the region of 1.2–2.1  $\mu\text{m}$ . We are developing hemispherical TPA Si photodetectors insensitive to polarization light.

**Acknowledgements** This work was supported by the National Natural Science Foundation of China, Program Nos. 60476027 and 60506016, and Collaborative projects of NSFC-RFBR agreement, Program Nos. 60711120182 and 60811120023.

## References

1. R. Soref, IEEE J. Sel. Top. Quantum Electron. **12**, 1678 (2006)
2. R.A. Soref, S.J. Emelett, W.R. Buchwald, J. Opt. A Pure Appl. Opt. **8**, 840 (2006)
3. Y. Takagi, T. Kobayashi, K. Yoshihara, Opt. Lett. **17**, 658 (1992)
4. F.R. Laughton, J.H. Marsh, D.A. Barrow, E.L. Portnoi, IEEE J. Quantum Electron. **30**, 838 (1994)
5. H.K. Tsang, L.Y. Chan, J.B.D. Soole, H.P. LeBlanc, M.A. Koza, R. Bhat, Electron. Lett. **31**, 1773 (1995)

6. J. Zhang, Q. Lin, G. Piredda, R.W. Boyd, G.P. Agrawal, P.M. Fauchet, *Appl. Phys. Lett.* **91**, 071113 (2007)
7. P.D. Maker, R.W. Terhune, *Phys. Rev.* **137**, A801 (1965)
8. T.K. Liang, H.K. Tsang, I.E. Day, J. Drake, A.P. Knights, M. Asghari, *Appl. Phys. Lett.* **81**, 1323 (2002)
9. C. Zhanguo, J. Gang, Y. Maobin, *J. Phys. D Appl. Phys.* **34**, 3078 (2001)
10. M. Sheik-Bahae, A.A. Said, T.H. Wei, D.J. Hagan, E.W. Van Stryland, *IEEE J. Quantum Electron.* **26**, 760 (1990)
11. R. DeSalvo, M. Sheik-Bahae, A.A. Said, D.J. Hagan, E.W. Van Stryland, *Opt. Lett.* **18**, 194 (1993)
12. C. Flytzanis, *Phys. Lett.* **31A**, 273 (1970)